Kobe University Repository : Kernel

PDF issue: 2025-01-10

# Highly Stable Vibration Measurements by Common-path off-axis Digital Holography

Kumar, Manoj

Pensia, Lavlesh

Kumar, Raj

(Citation)
Optics and Lasers in Engineering,163:107452

(Issue Date)
2023-01-03

(Resource Type)
journal article

(Version)
Accepted Manuscript

(Rights)
© 2022 Elsevier Ltd. All rights reserved.
Creative Commons Attribution-NonCommercial-NoDerivs

(URL)
https://hdl.handle.net/20.500.14094/0100488723

KOBE UNIVERSITY

**Highlights:**

1. A novel configuration of a common-path off-axis digital holographic system, with high mechanical stability and compact in size, is proposed.
2. The decisive advantages of the proposed digital holographic systems are its very simple optical design, compact in size, less-vibration sensitive to external perturbations, and cost-effectiveness as uses fewer optical elements
3. The feasibility of the proposed system is demonstrated its capability for vibration measurements of 3D objects using a high-speed camera which is triggered to record the vibration of the object as a function of the time.
4. Due to its simple geometry and significant outcomes, the proposed system could be established as a powerful tool for a wide range of optical imaging and measurement investigations.

Manuscript File Click here to view linked References

# Highly Stable Vibration Measurements by Common-path off-axis Digital Holography

Manoj Kumar[1,2,*], Lavlesh Pensia[1,3], and Raj Kumar[1,3,**]

[1]CSIR-Central Scientific Instruments Organization, Sector 30C, Chandigarh 160030, India
[2]Graduate School of System Informatics, Department of System Science, Kobe University, Rokkodai 1-1, 657-8501, Japan
[3]Academy of Scientific and Innovative Research (AcSIR), Ghaziabad 201002, India
*manojklakra@gmail.com
**raj.optics@csio.res.in

## Abstract

Measurements of vibration and dynamic deformation with high resolution and accuracy by non-destructive techniques are of great interest in many branches of engineering. We report a non-destructive method based on digital holographic interferometry for high-precision micro-vibration measurement of a 3D object. Herein, a new and simple configuration of a common-path off-axis digital holographic system, with high mechanical stability and compact in size, is proposed. The simplicity, compactness, and high stability of the proposed setup are provided by employing a wedge plate in-line with the test object to create a clean reference beam. The object and reference beams propagate the same path, without the need for any specialized optical component or arrangement, and these beams allow to interfere on the faceplate of the image sensor. The feasibility of the proposed system is demonstrated by measuring the vibration of the objects driven by different excitation signals. A series of digital holograms of a vibrating object is recorded by the use of a high-speed image sensor. The result of the reconstruction of the recorded holograms is an array of complex numbers containing the complete amplitude and phase profile of the object, which in turn provides displacement and vibration information. Due to its simple geometry and significant outcomes, the proposed system could be established as a powerful tool for a wide range of optical imaging and measurement investigations.

**Keywords:** Digital holographic interferometry, Common-path configuration, Phase imaging, Vibration measurement.

## Introduction

Vibration, resulting from mechanical disturbances, is one of the most popular phenomena which exists everywhere and at all the times. Measurement of vibration is of great interest in various fields for monitoring the condition, operation, and fault diagnosis of machines and components. Vibration measurement and sensing technology have been experiencing rapid growth with the development of electronic, computer technology, and manufacturing processes, and accordingly, the measurement methods and the types of sensors are evolving and maturing. The vibration measurement methods are generally categorized into contact type [1,2] and non-contact type methods [3-27]. The contact type methods including the piezoelectric sensors, accelerometers, and transducers require to adhere to the chosen location on the vibrating surface and require time-consuming point-by-point scanning of the object. These sensors are difficult to apply on small objects and their mass can affect the vibration, even changing the vibration behavior. These limitations can be overcome by non-contact type optical methods. The optical-laser-based non-destructive methods are renowned and have drawn more attention because they provide full-field information non-intrusively with high resolution and accuracy, and these methods are fast and robust. The dynamic characteristics of the vibrating object are unaltered by these measurement processes as no added mass or forces are applied to the tested object. Several non-contact type methods have been developed that are established as powerful tools for non-destructive testing and evaluation. These methods include interferometry [3], Moiré interferometry [6-8], shearography [9], speckle interferometry [10-14], and holographic interferometry [15-27], to name a few.

Among these methods, holographic interferometry enjoys the virtues of being high measurement sensitivity and resolution, and therefore, has emerged as a strong candidate for non-destructive testing and industrial inspections [28]. Holographic interferometry for vibration measurement started with the pioneering work of Powell and Stetson [15,16], in 1965. As a result of this introductory contribution, a wide range of applications has been developed. The techniques and methods surrounding holography have continuously been refined and extended to cases of importance. Thanks to the advancement of new recording media such as CCD (charge-coupled device) and CMOS (complementary metal–oxide–semiconductor) cameras and digital image processing techniques, particularly at the beginning of the 1990s, leading to the development of digital holography [29]. Since then, this technology has been progressing rapidly in diverse fields [30-47], recounting the significant evidence of the method's popularity. The interest in vibration measurement by digital holographic systems is growing substantially over the years, and different techniques such as time-average [15-17], sideband [18, 19], double pulse [20], double exposure [21, 22], stroboscopic [23], hybrid [24, 25], and multiplexing [26, 27] digital holography, have been reported for this purpose.

A survey of the literature indicates that most of these reported works for vibration measurements employ complicated and bulkier optical arrangements which require precise alignment. Most of these digital holographic setups are based on Mach-Zehnder/Michelson-type two-channel configurations, where the object and reference beams propagate along different paths through different optical components. Due to which any slight disturbance such as mechanical vibrations or air turbulence occurring in either of the two-channels may lead to lowering the spatial and temporal phase stability, and hence affects the measurement accuracy. These shortcomings of the two-channel digital holographic interferometry can be overcome by introducing the common-path configuration of the optical setup. Recent years have witnessed many advances in the common-path configurations of digital holographic systems owing to their several advantages. In common-path configurations, both the object and reference beams follow almost the same path and stay fixed or change identically, therefore, providing higher temporal and spatial phase stability. These systems are simple and compact, however, they require special optical components or tricky optical designs to build them. Different common-path digital holographic systems for different investigations [48-58] have been reported in the literature.

In this paper, we propose a new common-path configuration of digital holography and demonstrated its capability for vibration measurements of 3D objects using a high-speed camera which is triggered to record the vibration of the object as a function of the time. It requires a camera frame rate higher than the vibration frequency in order to record sequential digital holograms to completely analyze the vibration motion of the test object. Upon reconstruction of the sequential digital holograms by an appropriate numerical reconstruction method, the spatial phase distributions can be retrieved which enables to measure instantaneous 3D surface profiling, deformation/displacement, and dynamic responses of the vibrating test object.

## Methodology

Generally, the reference beam is derived from the object beam in the common-path digital holographic geometries. In the self-referencing geometry of the common-path digital holographic systems [50-53], a portion of the object beam itself acts as the reference beam. Other geometries under common-path digital holographic systems employ some specialized optical components to divide the object beam into two beams where one of the beams is spatially filtered by a pinhole at its Fourier plane to generate a clean reference beam [48]. However, both geometries have some limitations, such as, in self-referencing geometry, the field-of-view is reduced significantly and the reference beam (which is the portion of the object beam) may contain object information and so the unwanted spatial phase variations, thus, it always requires a careful selection of a portion with no object information in it. The self-referencing geometries are useful for sparse objects only. On the other hand, in the latter case, a precise alignment of the pinhole and sufficiently high laser intensity, are required.

Here, the aforementioned limitations of the common-path geometries of digital holographic systems are overcome by proposing a new configuration of common-path digital holography. The new common-path off-axis configuration of digital holography is realized by employing a wedge plate in-line with the test object. The wedge plate is placed in the path of the illumination beam just before the test object (~ 5.5 cm) on a 2D translation stage and serves as to produce a without phase modulated reference beam by reflection from the front surface. The backscattered light from the object and the reference beam follow almost the same path to the image sensor where they interfere to form a digital hologram. The separation of the interfering beam paths is in the gap between the object surface and the wedge plate, which should be smaller than the coherence length of the laser light used in the experiment. Figure 1(a) shows the schematic of the proposed digital holographic setup. The geometry of the proposed setup is designed with collinear illumination and observation directions to have maximum sensitivity to out-of-plane displacement. A reflecting surface is used as an object which is driven by different excitation signals by a mobile phone (Redmi Note 5 Pro). A laser beam of wavelength 532 nm (coherence length = 100 meters) is expanded by the spatial filter assembly (with 40X microscopic objective and 5 μm pinhole) and collimated by using a lens ($f$ = 200 mm). The collimated light is allowed to incident on the beam splitter (50:50) at which the light is reflected towards the wedge plate (wedge angle, $\alpha = 5^{\circ}$) and test object. Two reflected beams are generated by the reflection from the front and rear surfaces of the wedge plate, as shown in Fig. 1(b), and propagate toward the image sensor (resolution- 768 × 512 pixels, pixel pitch 20μm at 50,400 fps) via the same beam splitter along with the backscattered object beam. The phenomenon of the generation of two reflected beams each from the front and rear surfaces of the wedge plate and the passing of the object beam through it, is schematically shown in Fig. 1(b). A *4f* (lenses of $f$ = 200 mm) system is used before the image sensor to filter out one of the reflected beams (from the back surface) at the Fourier plane of lens $L_1$, by inserting an aperture and another beam reflected from the front surface is used as the reference beam for hologram recording. The backscattered object and reference beam interfere to form the digital hologram at the faceplate of the image sensor. The off-axis configuration is achieved by tilting the wedge plate by a small angle. The intensity recorded on the image sensor is represented by

$$I_H(x,y) = |O_H(x,y)|^2 + |R_H(x,y)|^2 + R_H(x,y)O_H^*(x,y) + R_H^*(x,y)O_H(x,y) \qquad (1)$$

where, $O(x,y)$ and $R(x,y)$ are the object and reference waves, the subscript $H$ represents the hologram plane, and * denotes the complex conjugate.

In Eq. (1), the first two terms represent the zero-order term which doesn't contain phase information and is therefore not of interest in holography; and the last two terms contain the complete information of the object wave (i.e. the amplitude and phase) to form the real and virtual image of the object, respectively. The object's complete information from the

recorded hologram can be retrieved by spatial filtering using the Fourier-transform method [28]. By taking the Fourier transform of the recorded intensity, the last two terms of Eq. (1) are separated in the Fourier plane and appear as sidebands because of the off-axis angle between the object and reference waves. One of these terms is extracted by drawing a filtering mask and eliminating other terms, followed by an inverse Fourier transformation to obtain the complex amplitude of the wavefront, $O_H(\chi, \xi)$, where $\chi$ and $\xi$ are the coordinates in the reconstruction plane. From the complex amplitude, the phase of the wavefront is calculated by the relation,

$$\phi_H(\chi, \xi) = tan^{-1}\left[\frac{Im[O_H(\chi,\xi)]}{Re[O_H(\chi,\xi)]}\right] \tag{2}$$

where, *Im* and *Re* denote the imaginary and real parts respectively.

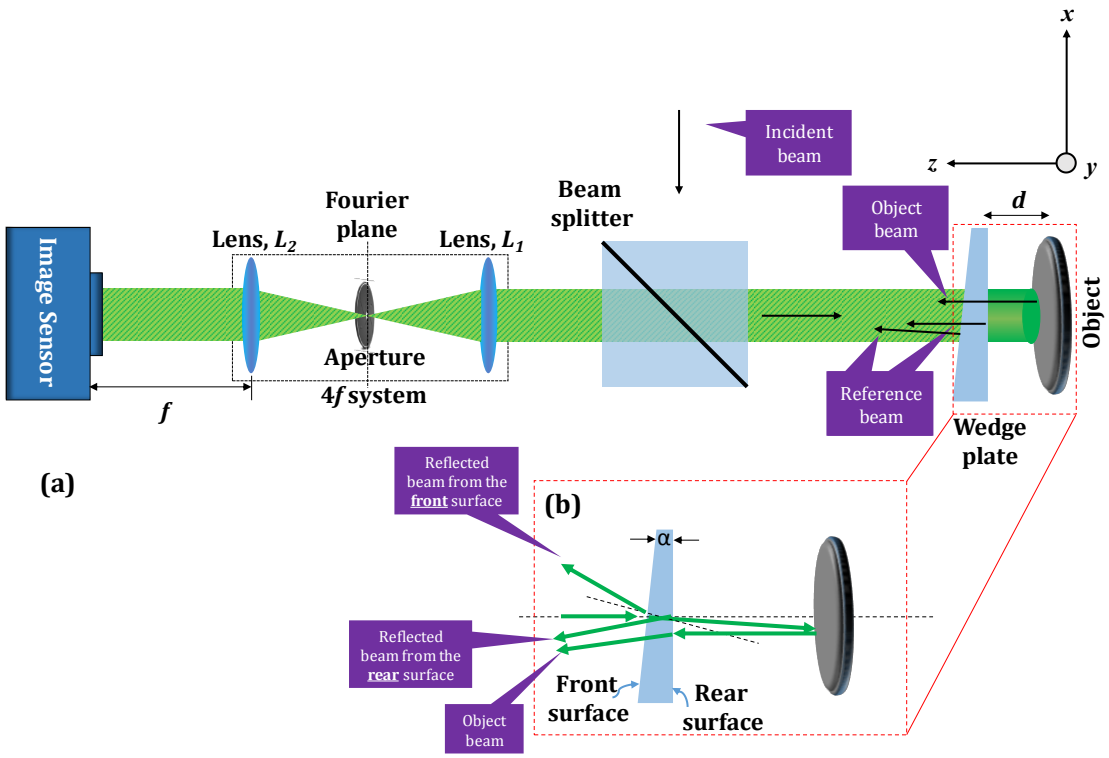


Fig. 1: (a) Schematic of the experimental setup and (b) schematic for explaining the generation of reflected beams and passing of object beam through the wedge plate.

A sequence of digital holograms is recorded by the high-speed image sensor with a frame rate higher than the vibration frequency of the test object. It should be noted that the frame rate should be two times higher than the vibration frequency, as it can be understood from the Nyquist- Shannon theorem. Each recorded hologram is processed to obtain the phase and then phase difference between the two wavefronts: one initially recorded (say at $t = t_0$) and

another at a time interval of $\Delta t$ (where $\Delta t$ is the time between the successive exposures), is calculated and expressed as

$$\Delta\phi_{H_{\Delta t,0}}(\chi,\xi) = \Delta\phi_{H_{\Delta t}}(\chi,\xi) - \Delta\phi_{H_0}(\chi,\xi) \tag{3}$$

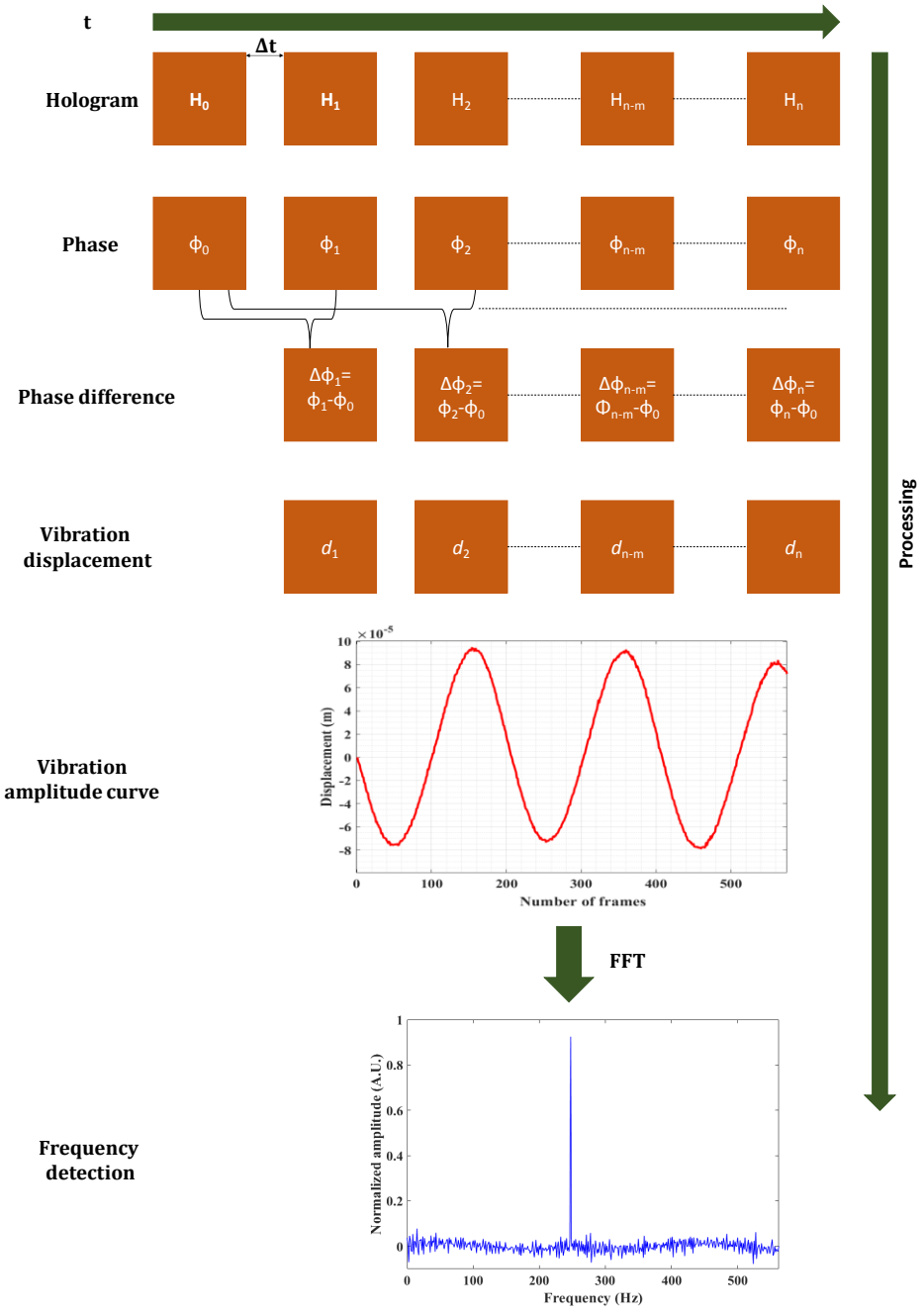


Fig. 2: Flow chart for calculating the instantaneous vibration displacement as a function of the time from a sequence of digital holograms recorded by using a high-speed sensor (FFT: fast Fourier transform).

The obtained phase difference is wrapped in the range $(-\pi, \pi)$ radian corresponding to the principal value of the arctan function, and an unwrapping algorithm is required to remove this phase discontinuity to obtain the continuous actual phase difference. The obtained actual phase difference is used to determine the out-of-plane displacement or instantaneous vibration displacement as

$$d(\chi, \xi) = \frac{\lambda}{4\pi} \Delta\phi_{H_{\Delta t,0}}(\chi, \xi) \tag{4}$$

Since the setup is designed to have collinear observation and illumination directions, therefore, it allows for maximum out-of-plane sensitivity. The same procedure is followed for all the recorded digital holograms of the vibrating test object to obtain the phase difference with respect to the initial phase $[\Delta\phi_{H_0}(\chi, \xi)]$. Therefore, the vibration displacement at any point within the measured region of the recorded digital hologram can be calculated and plotted as a vibration curve. A flow chart of the vibration measurement from the recorded sequential digital holograms is illustrated in Fig. 2.

## Experiments and Results

First, the performance of the proposed common-path digital holographic system is evaluated by measuring the temporal phase stability. The higher temporal stability of a holographic system demonstrates its capability to be resistant to external mechanical vibrations or air turbulence. The proposed system, owing to its common-path configuration, is expected to show higher temporal stability compared to the conventional two-channel configuration. The temporal stability of the system was measured by recording a time series of holograms (6000 holograms) at the rate of 60 frames per second, for 100 s without any vibration isolation. Then, each hologram is numerically reconstructed to extract the phase distributions, and the phase difference distributions are calculated by comparing the extracted phase distributions to that of the first recorded hologram. The standard deviation is calculated at each spatial location (175×175 pixel points) of every phase difference distribution, since the standard deviation of the time variation of phase distribution acts as the measure of fluctuation at that point. Figure 3 shows the histogram of the standard deviation indicating that a mean fluctuation is 0.0086 radian without the need for vibration isolation. The measured temporal stability of the proposed system is higher compared to traditional two-channel (e.g., Mach–Zehnder) digital holographic system (~0.2 radians) as reported in [48].

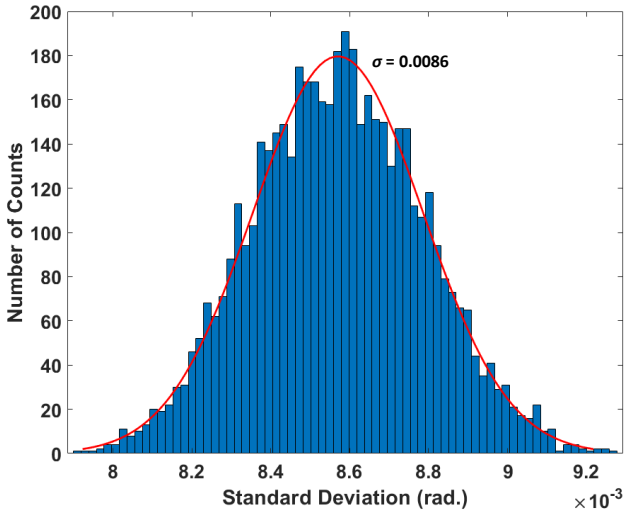


Fig. 3: Temporal stability of the proposed setup. Histogram of the standard deviation of the reconstructed phase distributions for a defined spatial location.

In order to prove the capability of the proposed system for dynamic events or vibration measurement, an experiment was performed in which a series of holograms at the frame rate of 40,000 frames per second are recorded by the high-speed camera [Resolution- 1024 x 512, pixel pitch- 20μm x 20μm], when the object is vibrating with a frequency of 248 Hz. A metallic reflecting surface is used as an object which is driven by a standard sinusoidal signal at the frequency of 248 Hz. The recorded digital holograms are numerically reconstructed by the Fresnel diffraction method as discussed in the previous section to extract the phase distribution and finally the vibration displacement as a function of the time. Figures 4(a-b) show the recorded digital holograms at two-time instances and their Fourier spectra are shown in Figs. 4(c-d), respectively. The extracted wrapped phase difference map and corresponding unwrapped phase map are shown, respectively, in Figs. 4(e-f). The unwrapped phase map is obtained by using the PUMA phase unwrapping algorithm [59]. From the obtained unwrapped phase maps, vibration displacement at a pixel location [$(\chi,\xi)$ = (190,160)] within the measured region, is calculated for the 575 digital holograms, and plotted as a vibration curve, as shown in Fig. 4(g). In Fig. 4(g), 575 frames are equivalent to 14.375 ms. The frequency of the vibrating objects can be measured by implementing the Fourier transform to the displacement values for each frame. Figure 4(h) shows the measured frequency at 248 Hz of the vibrating object. Several experiments were performed to verify the vibration measurement capability of the proposed highly stable digital holographic system at different vibration frequencies of the object. Figure 5 shows the measured vibration curve within the measured region [at a pixel location $(\chi,\xi)$ = (150,150)] and the detected frequency at 498 Hz of the vibrating object.

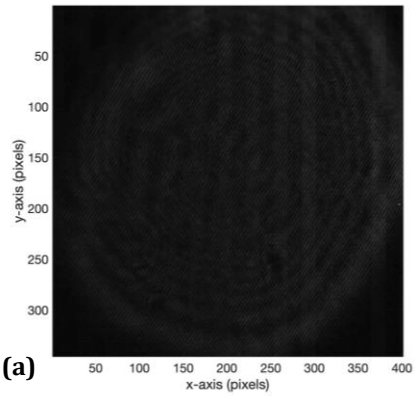
y-axis (pixels)
50
100
150
200
250
300
x-axis (pixels)
50
100
150
200
250
300
350
400

**(a)**

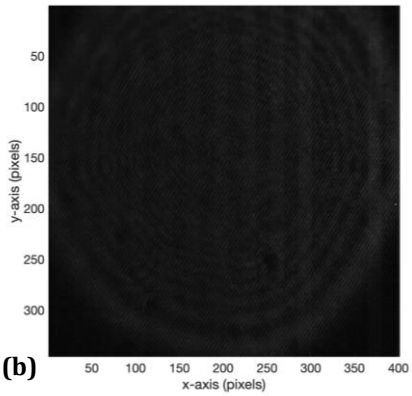
y-axis (pixels)
50
100
150
200
250
300
x-axis (pixels)
50
100
150
200
250
300
350
400

**(b)**

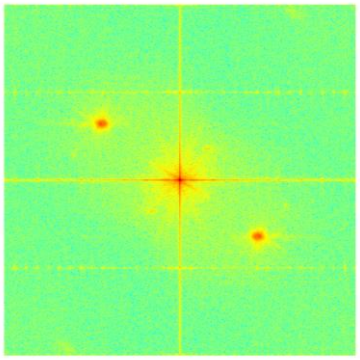

**(c)**

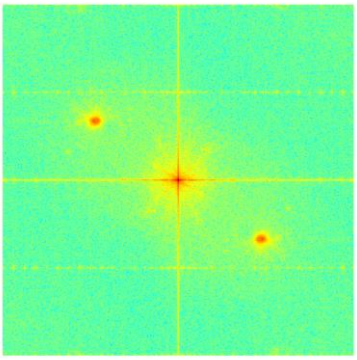

**(d)**

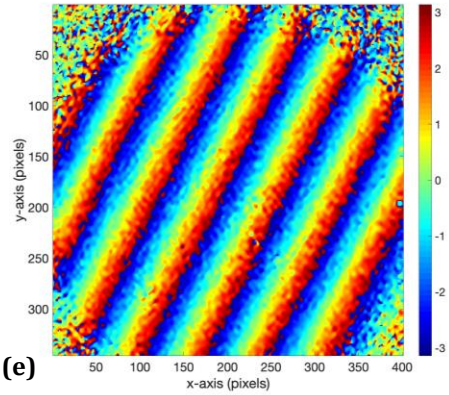
y-axis (pixels)
50
100
150
200
250
300
x-axis (pixels)
50
100
150
200
250
300
350
400
3
2
1
0
-1
-2
-3

**(e)**

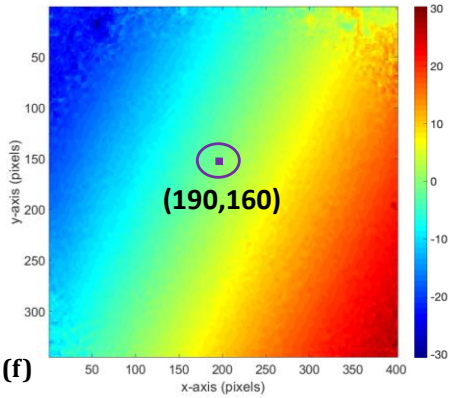
(190,160)
y-axis (pixels)
50
100
150
200
250
300
x-axis (pixels)
50
100
150
200
250
300
350
400
30
20
10
0
-10
-20
-30

**(f)**

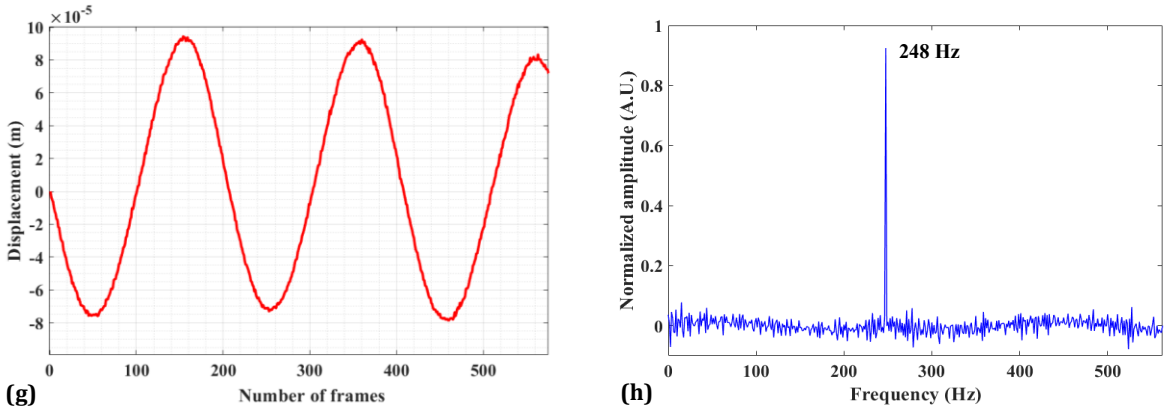


Fig. 4: (a), (b) Recorded holograms at two instants of time; (c), (d) Fourier spectra of (a) (b); (e), (f) retrieved wrapped and corresponding unwrapped phase maps, (g) vibration amplitude-time curve at a position with pixel location (χ, ξ) = (190, 160) as marked in (f), and (h) plot of detected frequency at 248 Hz.

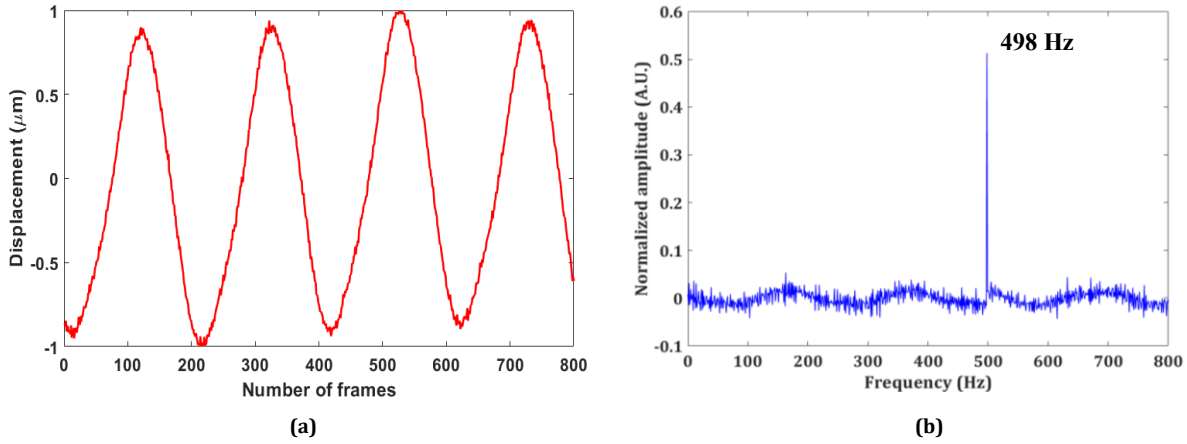


Fig. 5: (a) Vibration amplitude-time curve and (b) plot of detected frequency at 498 Hz.

In the second experiment, a 3D or multiplane object is considered as a vibrating object. The object is made by adhering three metallic step surfaces (A, B, and C) with an axial separation of about 5 mm from each other, as depicted in Fig. 6. This object is driven by a periodic signal of frequency 248 Hz. A time series of digital holograms are recorded by the high-speed image sensor at 50400 frames/sec for 0.2 seconds. A recorded digital hologram is first processed to obtain the complex amplitude, and it is propagated to the appropriate distance, i.e. to the image plane of interest of the three surfaces by the angular spectrum method [29, 47]. Figures 7(a-e) show the retrieved amplitude images of the multi-plane object (the three surfaces are marked with numbers 1, 1, and 1.11, respectively) at different reconstruction distances. Figures 7(a), (b), and (c), show the three in-focus planes, as marked by the dotted red color rectangular boxes, of the multiplane object that are obtained at the reconstruction distances of 4 mm, 5 mm, and 6 mm, respectively. The corresponding phase images at the reconstruction distances of 4 mm, 5 mm, and 6 mm, are shown in Figs. 7(d-f). The

coordinates for three in-focus planes, obtained at the reconstructed distances of 4 mm, 5 mm, and 6 mm, are ($\chi'$, $\xi'$), ($\chi''$, $\xi''$), and ($\chi'''$, $\xi'''$), respectively. For the in-focus plane at the reconstruction distance of 4 mm, the time series digital holograms (1000 holograms) are then processed to obtain the phase difference. Finally, the vibration displacement at a point with pixel location ($\chi'$, $\xi'$) = (111, 138), within the measured region, is computed and plotted as a function of the number of frames (or time) as shown in Fig. 8 (a). Similarly, the vibration displacements at particular points [($\chi''$, $\xi''$) = (320, 135) and ($\chi'''$, $\xi'''$) = (532, 132)] on the other two axially separated in-focus planes, obtained at the reconstruction distances of 5 mm and 6 mm, respectively, are measured and plotted as shown respectively in Figs. 8(b) and (c).

The obtained results authenticate the feasibility of the proposed common-path off-axis high-speed digital holographic system for the measurement of dynamic events of 3D objects. Several experiments were performed to confirm the vibration-detecting capability of the proposed system with vibrating test objects up to frequencies of tens kHz. The system can be used for measuring displacement vibrations of most of the vibrating test objects with known, unknown, and random frequencies. In the future, the scope of the proposed technique will be further widened by measuring the sound field and ultrasound frequency.

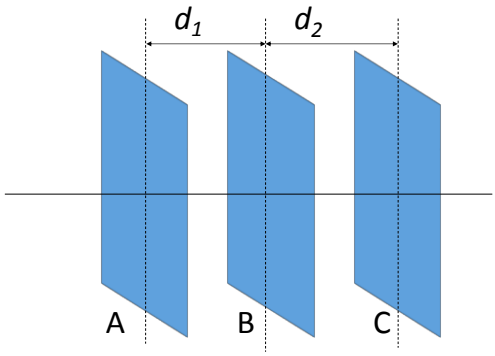


Fig. 6: Schematic of 3D (multiplane) object ($d_1 = d_2 = 5$ mm).

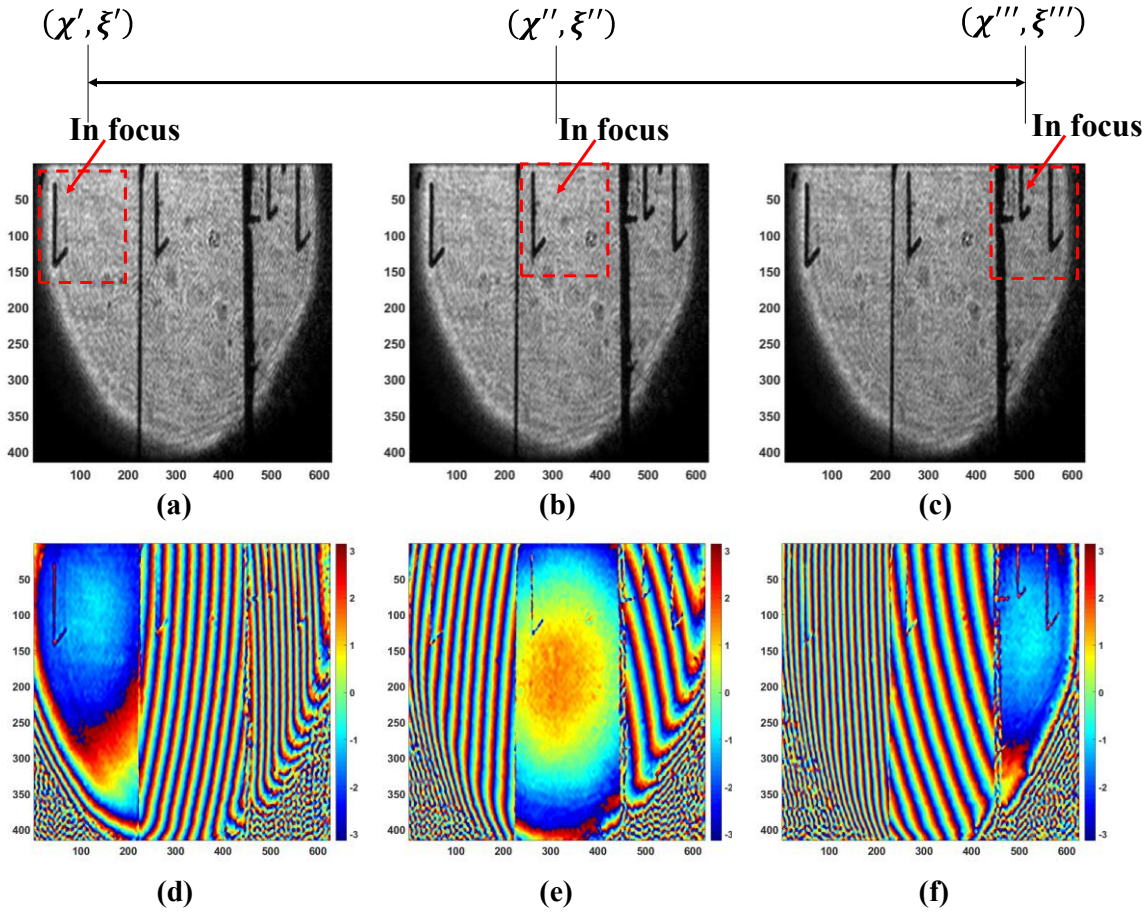


Fig. 7: Reconstructed amplitude and phase map results of the vibrating 3D object: (a-e) the reconstructed amplitude images at different in-focus image planes, and (f-j) corresponding phase maps.

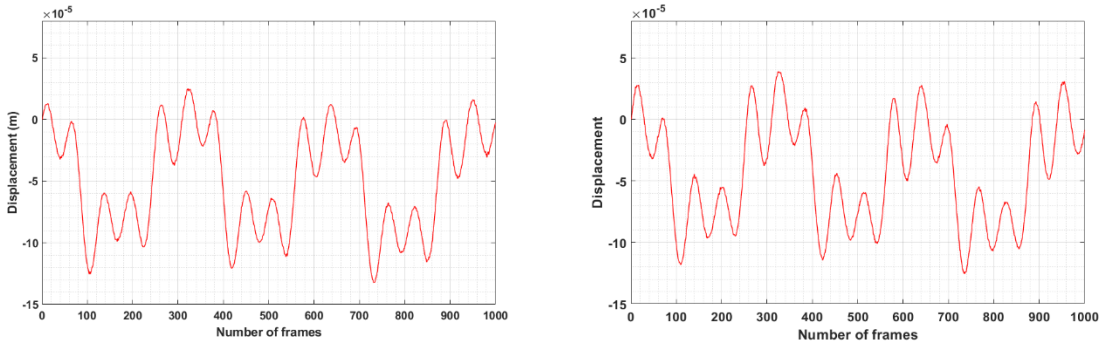


(a) (b)

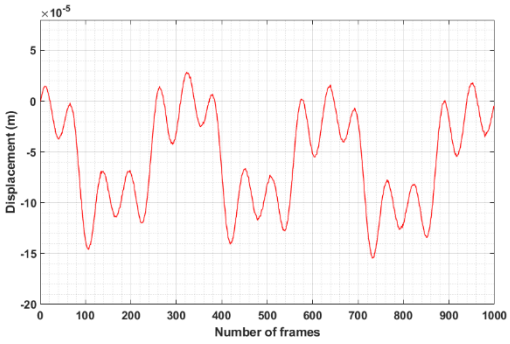


(c)

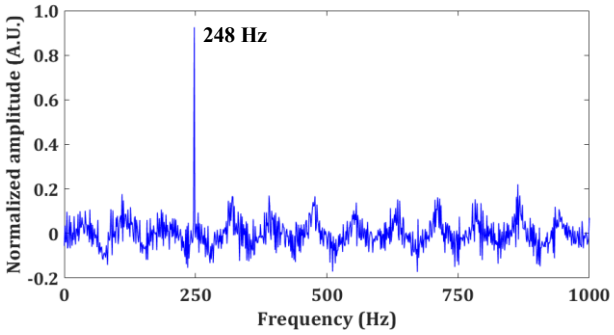


(d)

Fig. 8: Measured vibration amplitude-time curves, at three in-focus image planes obtained at the reconstruction distances of (a) 4 mm at a position [$\chi'$, $\xi'$ = (111, 138)]; (b) 5 mm at a position [$\chi''$, $\xi''$ = (320, 135)]; (c) 6 mm at a position [$\chi'''$, $\xi'''$ = (532, 132)]; and (d) plot of detected frequency.

## Conclusion

We have proposed a novel common-path off-axis digital holographic system by employing a wedge plate in-line with the test object and demonstrated it for evaluating the vibration measurement of 2D and 3D objects. The reflected light beam from the wedge plate produces a without phase modulated reference beam which interferes with the backscattered object beam. A time series of digital holograms, at a frame rate higher than the vibration frequency of the test objects, is recorded and processed to obtain the displacement vibration of the test object. The obtained results corroborate the feasibility of the system and its high temporal phase stability suggests that it could be well suited for 2D or 3D analysis of transient vibration in an industrial environment in which the measurement conditions are not ideal. The decisive advantages that distinguish it from other digital holographic systems are its very simple optical design, compact in size, less-vibration sensitive to external perturbations, and cost-effectiveness as uses fewer optical elements. Moreover, the system provides a field-of-view

as wide as that Mach-Zehnder/Michelson-type two-channel digital holographic systems. The system yields high temporal phase stability ~ 23 times higher than a two-channel digital holographic system. The proposed system overcomes several limitations of the common-path geometries of digital holographic systems and its simple design could even potentially allow for the development of a portable device for dynamic deformation and vibration measurements. These advantages of the proposed digital holographic system make it a suitable candidate for various applications.

**Funding**: The research work is financially supported by the CSIR, India under project number MLP 2014, and Lavlesh Pensia thanks CSIR, India for providing a fellowship to carry out this research work

**References:**

1. Figliola, Richard S. and Beasley, Donald E., "Measurement of Acceleration and Vibration," Theory and Design for Mechanical Measurement, 3rd ed., John Wiley & Sons, New York, 2000, pp. 482-488.
2. Dionisio, R., Torres, P., Ramalho, A., & Ferreira, R. (2021). Magnetoresistive sensors and piezoresistive accelerometers for vibration measurements: A comparative study. Journal of Sensor and Actuator Networks, 10(1), 22.
3. Bruce, C. F., Macinante, J. A., & Kelly, J. C. (1951). Vibration measurement by interferometry. Nature, 167(4248), 520-521.
4. Huang, S. R., Lerner, R. M., & Parker, K. J. (1992). Time domain Doppler estimators of the amplitude of vibrating targets. The Journal of the Acoustical Society of America, 91(2), 965-974.
5. Tapson, J. (1995). High precision, short range ultrasonic sensing by means of resonance mode-locking. Ultrasonics, 33(6), 441-444.
6. Harding, K. G., & Harris, J. S. (1983). Projection moiré interferometer for vibration analysis. Applied Optics, 22(6), 856-861.
7. Ritter, R., & Meyer, H. J. (1980). Vibration analysis of plates by a time-averaged projection-moiré method. Applied Optics, 19(10), 1630-1633.
8. Kafri, O., Band, Y. B., Chin, T., Heller, D. F., & Walling, J. C. (1985). Real-time moire vibration analysis of diffusive objects. Applied optics, 24(2), 240-242.
9. Yang, L., Steinchen, W., Kupfer, G., Mäckel, P., & Vössing, F. (1998). Vibration analysis by means of digital shearography. Optics and lasers in engineering, 30(2), 199-212.
10. Chiang, F. P., & Juang, R. M. (1976). Vibration analysis of plate and shell by laser speckle interferometry. Optica Acta, 23, 997-1009.
11. Petzing, J. N., & Tyrer, J. R. (1998). Recent developments and applications in electronic speckle pattern interferometry. The Journal of Strain Analysis for Engineering Design, 33(2), 153-169.
12. Ellingsrud, S., & Rosvold, G. O. (1992). Analysis of a data-based TV–holography system used to measure small vibration amplitudes. JOSA A, 9(2), 237-251.
13. Koyuncu, B., & Cookson, J. (1980). Semi-automatic measurements of small high-frequency vibrations using time averaged electronic speckle pattern interferometry. Journal of Physics E: Scientific Instruments, 13(2), 206.
14. Rosvold, G. O., & Løkberg, O. J. (1993). Effect and use of exposure control in vibration analysis using TV holography. Applied optics, 32(5), 684-691.
15. Stetson, K. A., & Powell, R. L. (1965). Interferometric hologram evaluation and real-time vibration analysis of diffuse objects. JOSA, 55(12), 1694-1695.
16. Powell, R. L., & Stetson, K. A. (1965). Interferometric vibration analysis by wavefront reconstruction. JOSA, 55(12), 1593-1598.
17. Picart, P., Leval, J., Mounier, D., & Gougeon, S. (2003). Time-averaged digital holography. Optics letters, 28(20), 1900-1902.

18. Aleksoff, C. C. (1971). Temporally modulated holography. Applied Optics, 10(6), 1329-1341.
19. Joud, F., Laloë, F., Atlan, M., Hare, J., & Gross, M. (2009). Imaging a vibrating object by sideband digital holography. Optics express, 17(4), 2774-2779
20. Pedrini, G., Zou, Y. L., & Tiziani, H. J. (1995). Digital double-pulsed holographic interferometry for vibration analysis. Journal of Modern Optics, 42(2), 367-374.
21. Pedrini, G., Osten, W., & Gusev, M. E. (2006). High-speed digital holographic interferometry for vibration measurement. Applied optics, 45(15), 3456-3462.
22. Fu, Y., Pedrini, G., & Osten, W. (2007). Vibration measurement by temporal Fourier analyses of a digital hologram sequence. Applied optics, 46(23), 5719-5727.
23. De Greef, D., Soons, J., & Dirckx, J. J. (2014). Digital stroboscopic holography setup for deformation measurement at both quasi-static and acoustic frequencies. International Journal of Optomechatronics, 8(4), 275-291.
24. Leval, J., Picart, P., Boileau, J. P., & Pascal, J. C. (2005). Full-field vibrometry with digital Fresnel holography. Applied optics, 44(27), 5763-5772.
25. Verpillat, F., Joud, F., Atlan, M., & Gross, M. (2012). Imaging velocities of a vibrating object by stroboscopic sideband holography. Optics express, 20(20), 22860-22871.
26. Picart, P., Leval, J., Pascal, J. C., Boileau, J. P., Grill, M., Breteau, J. M., ... & Gillet, S. (2005). 2D full field vibration analysis with multiplexed digital holograms. Optics express, 13(22), 8882-8892.
27. Kumar, M., & Matoba, O. (2021). 2D full-field displacement and vibration measurements of specularly reflecting surfaces by two-beam common-path digital holography. Optics Letters, 46(23), 5966-5969.
28. Sheridan, J. T., Kostuk, R. K., Gil, A. F., Wang, Y., Lu, W., Zhong, H., ... & Saravanamuttu, K. (2020). Roadmap on holography. Journal of Optics, 22(12), 123002.
29. Schnars, U., & Jüptner, W. (1994). Direct recording of holograms by a CCD target and numerical reconstruction. Applied optics, 33(2), 179-181.
30. Pedrini, G., & Tiziani, H. J. (1995). Digital double-pulse holographic interferometry using Fresnel and image plane holograms. Measurement, 15(4), 251-260.
31. Pedrini, G., Zou, Y. L., & Tiziani, H. J. (1997). Simultaneous quantitative evaluation of in-plane and out-of-plane deformations by use of a multidirectional spatial carrier. Applied optics, 36(4), 786-792.
32. Yamaguchi, I., Matsumura, T., & Kato, J. I. (2002). Phase-shifting color digital holography. Optics letters, 27(13), 1108-1110.
33. Awatsuji, Y., Fujii, A., Kubota, T., & Matoba, O. (2006). Parallel three-step phase-shifting digital holography. Applied Optics, 45(13), 2995-3002.
34. Kemper, B., Carl, D. D., Schnekenburger, J., Bredebusch, I., Schäfer, M., Domschke, W., & von Bally, G. (2006). Investigation of living pancreas tumor cells by digital holographic microscopy. Journal of biomedical optics, 11(3), 034005.
35. Tounsi, Y., Kumar, M., Siari, A., Mendoza-Santoyo, F., Nassim, A., & Matoba, O. (2019). Digital four-step phase-shifting technique from a single fringe pattern using Riesz transform. Optics Letters, 44(14), 3434-3437.
36. Kakue, T., Yonesaka, R., Tahara, T., Awatsuji, Y., Nishio, K., Ura, S., Kubota, T., & Matoba, O. (2011). High-speed phase imaging by parallel phase-shifting digital holography. Optics letters, 36(21), 4131-4133.
37. Solís, S. M., Santoyo, F. M., & del Socorro Hernández-Montes, M. (2012). 3D displacement measurements of the tympanic membrane with digital holographic interferometry. Optics express, 20(5), 5613-5621.
38. Kumar, M., Quan, X., Awatsuji, Y., Tamada, Y., & Matoba, O. (2020). Digital holographic multimodal cross-sectional fluorescence and quantitative phase imaging system. Scientific Reports, 10(1), 1-13.
39. Chowdhury, S., Eldridge, W. J., Wax, A., & Izatt, J. A. (2015). Spatial frequency-domain multiplexed microscopy for simultaneous, single-camera, one-shot, fluorescent, and quantitative-phase imaging. Optics letters, 40(21), 4839-4842.

40. Kumar, M., Pensia, L., & Kumar, R. (2022). Single-shot off-axis digital holographic system with extended field-of-view by using multiplexing method. Scientific Reports, 12(1), 1-10.
41. Khaleghi, M., Guignard, J., Furlong, C., & Rosowski, J. J. (2015). Simultaneous full-field 3-D vibrometry of the human eardrum using spatial-bandwidth multiplexed holography. Journal of biomedical optics, 20(11), 111202.
42. Kumar, M., & Shakher, C. (2016). Experimental characterization of the hygroscopic properties of wood during convective drying using digital holographic interferometry. Applied optics, 55(5), 960-968.
43. Kumar, M., Vijayakumar, A., & Rosen, J. (2017). Incoherent digital holograms acquired by interferenceless coded aperture correlation holography system without refractive lenses. Scientific Reports, 7(1), 1-11.
44. Kakue, T., Endo, Y., Nishitsuji, T., Shimobaba, T., Masuda, N., & Ito, T. (2017). Digital holographic high-speed 3D imaging for the vibrometry of fast-occurring phenomena. Scientific reports, 7(1), 1-10.
45. Merola, F., Memmolo, P., Miccio, L., Savoia, R., Mugnano, M., Fontana, A., ... & Ferraro, P. (2017). Tomographic flow cytometry by digital holography. Light: Science & Applications, 6(4), e16241-e16241.
46. Quan, X., Kumar, M., Matoba, O., Awatsuji, Y., Hayasaki, Y., Hasegawa, S., & Wake, H. (2018). Three-dimensional stimulation and imaging-based functional optical microscopy of biological cells. Optics letters, 43(21), 5447-5450.
47. Kumar, R., Dwivedi, G., & Singh, O. (2021). Portable digital holographic camera featuring enhanced field of view and reduced exposure time. Optics and Lasers in Engineering, 137, 106359.
48. Kumar, M., Quan, X., Awatsuji, Y., Cheng, C., Hasebe, M., Tamada, Y., & Matoba, O. (2020). Common-path multimodal three-dimensional fluorescence and phase imaging system. Journal of biomedical optics, 25(3), 032010.
49. Rajput, S. K., Matoba, O., Kumar, M., Quan, X., & Awatsuji, Y. (2021). Sound wave detection by common-path digital holography. Optics and Lasers in Engineering, 137, 106331.
50. Qu, W., Bhattacharya, K., Choo, C. O., Yu, Y., & Asundi, A. (2009). Transmission digital holographic microscopy based on a beam-splitter cube interferometer. Applied optics, 48(15), 2778-2783.
51. Chhaniwal, V., Singh, A. S., Leitgeb, R. A., Javidi, B., & Anand, A. (2012). Quantitative phase-contrast imaging with compact digital holographic microscope employing Lloyd's mirror. Optics letters, 37(24), 5127-5129.
52. Hsu, W. C., Su, J. W., Tseng, T. Y., & Sung, K. B. (2014). Tomographic diffractive microscopy of living cells based on a common-path configuration. Optics letters, 39(7), 2210-2213.
53. Singh, A. S., Anand, A., Leitgeb, R. A., & Javidi, B. (2012). Lateral shearing digital holographic imaging of small biological specimens. Optics express, 20(21), 23617-23622.
54. Kumar, M., Matoba, O., Quan, X., Rajput, S. K., Awatsuji, Y., & Tamada, Y. (2021). Single-shot common-path off-axis digital holography: applications in bioimaging and optical metrology. Applied Optics, 60(4), A195-A204.
55. Sun, T., Zhuo, Z., Zhang, W., Lu, J., & Lu, P. (2018). Single-shot interference microscopy using a wedged glass plate for quantitative phase imaging of biological cells. Laser Physics, 28(12), 125601.
56. Ebrahimi, S., Dashtdar, M., Sánchez-Ortiga, E., Martínez-Corral, M., & Javidi, B. (2018). Stable and simple quantitative phase-contrast imaging by Fresnel biprism. Applied Physics Letters, 112(11), 113701.
57. Kumar, M., Quan, X., Awatsuji, Y., Tamada, Y., & Matoba, O. (2020). Single-shot common-path off-axis dual-wavelength digital holographic microscopy. Applied Optics, 59(24), 7144-7152.
58. Kumar, M., Matoba, O., Quan, X., Rajput, S. K., Morita, M., & Awatsuji, Y. (2022). Quantitative dynamic evolution of physiological parameters of RBC by highly stable digital holographic microscopy. Optics and Lasers in Engineering, 151, 106887.
59. Bioucas-Dias, J. M., & Valadao, G. (2007). Phase unwrapping via graph cuts. IEEE Transactions on Image processing, 16(3), 698-709.

## Declaration of Competing Interest

The authors declare that they have no known competing financial interests or personal relationships that could have appeared to influence the work reported in this paper.